Mutations at a Glycine Loop in Aminolevulinate Synthase Affect Pyridoxal Phosphate Cofactor Binding and Catalysis†

Jian Gong,‡,§ Christopher J. Kay,‡ Michael J. Barber,‡,|| and Gloria C. Ferreira*,‡,||,⊥

Department of Biochemistry and Molecular Biology, College of Medicine, Institute for Biomolecular Science, and H. Lee Moffitt Cancer Center and Research Institute, University of South Florida, Tampa, Florida 33612

Received June 3, 1996⊗

ABSTRACT: 5-Aminolevulinate synthase catalyzes the first step of the heme biosynthetic pathway in animals, fungi, and some bacteria. The enzyme belongs to a large family of enzymes that use pyridoxal 5′-phosphate as an essential cofactor. We previously analyzed the informational content contained in each residue of a conserved glycine loop, which we proposed to form part of the cofactor binding site [Gong, J., & Ferreira, G. C. (1995) *Biochemistry 34*, 1678−1685]. We found that Gly-142 and −144 contain high informational content, and we identified G144A, G144S, G144T, and G142C as functional mutants. Here, the catalytic parameters, cofactor affinities, and spectral and thermostability properties of these four glycine mutants are determined to examine the function of the glycine loop. In addition, computer models of the glycine loops from the wild-type and mutant enzymes were generated, using glycogen phosphorylase *b* as the structural template. G144A, G144S, G144T, and G142C displayed lower affinity than the wild-type enzyme for the cofactor, reflected in the 8.5-, 8-, 24.5-, and 15-fold increases, respectively, in the dissociation constant value for binding of the cofactor. While the turnover numbers for G144A, G144S, G144T, and G142C were 43%, 39%, 21%, and 6% of the wild-type value, respectively, the K_m values for both substrates remained unchanged, with the exception of the G142C K_m^{Gly}, which showed a 4-fold increase. The UV−visible and CD spectra of Gly-144 mutants were similar to those of the wild type; however, the spectral properties of G142C suggest that this mutant binds the cofactor in a different mode at the active site. G144A, G144S, G144T, and G142C were also found to be less stable than the wild-type enzyme, with the thermotransition temperature, $T_{1/2}$, determined to be 3.5, 3, 3.5, and 5 °C, respectively, lower than that of the wild-type enzyme. Collectively, computer modeling of the wild-type and mutant forms of the ALAS glycine loop and biochemical and spectroscopic characterization of G144A, G144S, G144T, and G142C strongly suggest that the conserved glycine loop in 5-aminolevulinate synthase is a pyridoxal 5′-phosphate cofactor binding motif.

5-Aminolevulinate synthase (ALAS)[1] (EC 2.3.1.37) catalyzes the first step of heme biosynthesis in animals, fungi, and some bacteria (Jordan, 1991). The reaction involves the condensation of glycine and succinyl-CoA, which is the rate-limiting step in the liver and possibly in differentiating erythrocytes (Jordan, 1991). In animals, there are two isoforms of the enzyme, ALAS1, the hepatic or housekeeping form, and ALAS2, the erythroid-specific form. The two isoforms are encoded by distinct genes located on different chromosomes (Riddle et al., 1989) [for a recent review on ALAS, see Ferreira and Gong (1995)].

Like many other enzymes catalyzing reactions of amino acids, ALAS employs pyridoxal 5′-phosphate (PLP) as an essential cofactor. PLP is unique in its catalytic versatility as it participates in a wide variety of reactions catalyzed by a large family of PLP-dependent enzymes. Remarkably, nearly all of these enzymes use PLP as a cofactor to act on amino acid substrates. To date, the mystery of the ubiquity and versatility of the PLP cofactor is not fully solved, nor is a general picture of the PLP-binding site available for this large family of enzymes. Therefore, the study of ALAS structure/function will not only expand knowledge of ALAS and heme biosynthesis in general but, at the same time, it should also contribute to our understanding of the important PLP−enzyme family. Recently, residues and motifs involved in binding and orienting the cofactor in the ALAS active site have started to be unveiled. Lys-313 in murine ALAS2 was identified to form the Schiff base linkage with PLP (Ferreira et al., 1993). In addition, we recently proposed that a glycine loop (141-HGAGAGGTRNI in murine ALAS2) constitutes part of the PLP-binding site (Gong & Ferreira, 1995). This glycine-rich sequence is conserved in all ALAS known sequences (Gong & Ferreira, 1995). Importantly, a similar glycine-rich motif is present at the cofactor binding site in most PLP-dependent enzymes with available X-ray structures (Weber et al., 1978; Hyde et al., 1988; Kirsch et al., 1984; Antson et al., 1993; Toney et al., 1995; Momany et al., 1995). Moreover, it has been well established that

† This work was supported by the National Science Foundation (Grant MCB-9206574 to G.C.F.) and the National Institutes of Health (Grant GM32696 to M.J.B).

* To whom correspondence should be addressed. Tel: (813) 974-5797. Fax: (813) 974-5798. Email: gferreir@com1.med.usf.edu.

‡ Department of Biochemistry and Molecular Biology, College of Medicine.

§ American Heart Association Predoctoral Fellow, Florida Division (93GSF/9).

|| Institute for Biomolecular Science, H. Lee Moffitt Cancer Center and Research Institute.

⊥ American Cancer Society Junior Faculty Awardee (JFRA-401).

⊗ Abstract published in *Advance ACS Abstracts,* October 1, 1996.

[1] Abbreviations: ALAS, 5-aminolevulinate synthase; PLP, pyridoxal 5′-phosphate; EDTA, ethylenediamine tetraacetate; PMSF, phenylmethanesulfonyl fluoride; NTA, nitrilotriacetic acid; SDS, sodium dodecyl sulfate; SDS−PAGE, SDS−polyacrylamide gel electrophoresis; BSA, bovine serum albumin; Hepes, *N*-(2-hydroxyethyl)piperazine-*N*′-(2-ethanesulfonic acid); CD, circular dichroism; cvff, consistent valence force field; GPB, glycogen phosphorylase *b*.

S0006-2960(96)01296-2 CCC: $12.00

the consensus glycine-rich sequence GXGXXG is found in the region of (pyro)phosphate binding of numerous nucleotide-binding proteins (Saraste et al., 1990).

We previously performed an informational content analysis of each residue within the glycine-loop motif in murine ALAS2 (Gong & Ferreira, 1995). The partial random mutagenesis results revealed that most residues in the glycine loop could tolerate several other amino acid replacements. However, Gly-142 and Gly-144 could only tolerate alanine substitution, and Arg-149 was conserved in all the functional mutants. To further challenge the stringency of the two glycine positions, we constructed a codon-specific, 100% random library of Gly-142 and −144, and identified G142C, G144A, G144S, and G144T as the functional replacements. In the current study, we report the kinetic and spectroscopic characterization results of the above four glycine mutants, which provide new information about the contribution of the glycine loop in the ALAS cofactor binding site. In addition, we report the results of computer modeling of the ALAS glycine loop in the PLP-binding site, using glycogen phosphorylase *b* (GPB) as the structural template.

EXPERIMENTAL PROCEDURES

Materials

Restriction enzymes and T_4 DNA ligase were obtained from New England Biolabs and were used according to the manufacturer's instructions. The GeneClean II kit was the product of Bio 101 Inc. Deoxy- and dideoxynucleotide triphosphates were from United States Biochemical Corp. [α-^{35}S]dATP was from Du Pont/NEN Research Products. All the chemicals were purchased from Sigma or Fisher and were of the highest purity available. Ultrogel AcA 44 was obtained from IBF Biotechnics Inc., and DEAE-Sephacel was from Sigma. Ni^{2+}−NTA−agarose was ordered from Qiagen. Acrylamide and gel reagents were purchased from Bio-Rad. Centricon concentrators and Amicon ultrafiltration cells were obtained from Amicon. The bicinchoninic acid protein assay reagents were purchased from Pierce Chemical Co.

Methods

Mutagenesis, Expression, and Purification of G142C, G144A, G144S, and G144T. G142C, G144A, G144S, and G144T were the total functional replacements obtained from the random glycine library of the mature murine ALAS2, as previously reported (Gong & Ferreira, 1995). Wild-type and the mutant forms of ALAS were produced from expression plasmids containing their cDNAs under the control of the alkaline phosphatase promoter, which is induced by limited concentration of phosphate (Ferreira et al., 1993). The ALAS wild-type and mutant enzymes (*i.e.*, G142C, G144A, G144S, and G144T) were overexpressed in host *Escherichia coli* DH5α strain harboring the different expression plasmids, as previously described for the wild-type enzyme (Ferreira & Dailey, 1993). Purification of the Gly-144 mutants followed essentially the same procedure as described for the wild-type enzyme in Ferreira and Dailey (1993). Buffer A (20 mM potassium phosphate, pH 7.2, containing 1 mM EDTA, 5 mM β-mercaptoethanol, 10% glycerol, and 20 μM PLP) was used throughout the purification and the subsequent characterization experiments unless otherwise stated.

As the G142C mutant ALAS was largely insoluble when overexpressed in *Escherichia coli* DH5α cells; purification of this mutant using the above-mentioned method proved to be unsuccessful. Nickel chelate−agarose chromatography was utilized as an alternative to purify the G142C mutant ALAS. To this end, plasmid pJG10 was constructed. The pJG10 plasmid encodes the G142C mutant ALAS with an N-terminal extension of five histidine residues. A DNA fragment encoding a Gly-142 to Cys mutation was retrieved from the previously obtained G142C mutant plasmid, upon digestion with *Blp*I and *Xba*I. The fragment was purified from an agarose gel and ligated into the pDT6 (Tan & Ferreira, 1996), previously digested with the same two enzymes. The pDT6 plasmid contains a full-length mouse erythroid ALAS sequence with a five histidine tag at the N-terminus (Tan & Ferreira, 1996). The pJG10 construct was verified by restriction enzyme mapping and by sequencing according to the dideoxy-chain termination method (Sanger et al., 1977).

The G142C mutant ALAS was purified from pJG10 overexpressed in *E. coli* cells. Essentially, DH5α cells harboring pJG10 were grown in low phosphate medium containing 100 μg/mL ampicillin at 37 °C for 20 h, as described previously (Ferreira & Dailey, 1993). The subsequent purification was carried out at 4 °C. Cells were harvested by centrifugation. The cell pellet was then resuspended in buffer B, which contains 20 mM Tricine at pH 8.0, 5 mM β-mercaptoethanol, 10% glycerol, and 20 μM PLP. PMSF (100 μM) and 1 μg/mL each of aprotinin, leupeptin, and pepstatin were added to prevent proteolysis. The cells were broken by two passages through a French press at 10 000 psi. The cell debris was removed by centrifugation, and the supernatant, typically around 100 mL from 20 g of cell paste, was loaded onto a Ni^{2+}−NTA−agarose column (1.5 × 15 cm), previously equilibrated with buffer B. The column was washed successively with 5 bed volumes of buffer B, 5 bed volumes of buffer B containing 0.5 M NaCl, and 5 bed volumes of buffer B. Subsequently, the enzyme was eluted with 100 mM imidazole buffer, pH 7.2, containing 5 mM β-mercaptoethanol and 10% glycerol. The elution fractions were examined by SDS−PAGE and ALAS activity assay. Subsequently, the fractions containing ALAS were precipitated with 40% (w/v) ammonium sulfate and resuspended in buffer A as described earlier. The enzyme sample was dialyzed against buffer A to remove the residual ammonium sulfate salt. The dialysis typically proceeded for 5−6 h with three changes of buffer.

SDS-PAGE and Protein Determination. SDS−PAGE was performed as described by Laemmli (1970); 15% acrylamide and 1.5 mm thick gels were used. Aliquots of the protein samples (10−15 μL) were heated for 3 min at 95 °C in SDS−mercaptoethanol loading buffer, and the proteins were visualized upon Coomassie brilliant blue (R-250) staining. Protein concentrations were determined by the bicinchoninic acid assay, following Pierce's Application Note 13 as the protocol. Briefly, 50 μL of each protein sample was precipitated with 200 μL of cold acetone and then resuspended in 50 μL of deionized water. Subsequently, 1 mL of the BCA working reagent was added to each sample. After incubation at 37 °C for 30 min, the absorbance of each sample was recorded at 562 nm, using the blank as the reference. BSA was used as the standard and was treated exactly the same way as the samples.

Enzyme Assay and Analysis of the Kinetic Data. ALAS enzyme activity was measured by a continuous spectropho-

tometric assay as previously described (Hunter & Ferreira, 1995). The k_{cat} and K_m values for the wild-type and mutant forms of ALAS were determined as reported in Ferreira and Dailey (1993).

Preparation of Apo ALAS Enzyme. Apoenzymes, of both the wild-type and the mutant forms, were obtained through extensive dialysis. All ALAS samples were diluted to around 4 μM for subsequent dialysis, as higher enzyme concentration could cause protein precipitation during dialysis. The dialysis was carried out at 4 °C. The enzymes were dialyzed against at least 10 times enzyme sample volumes of buffer A without PLP, with multiple changes of the buffer throughout the dialysis. Activity assay and UV−visible spectra recording were performed to monitor the dialysis process, since it has been reported that apo ALAS is inactive and lacks the 420 nm peak, which corresponds to the Schiff base formed between the enzyme and the cofactor (Ferreira & Dailey, 1993). Finally, the apo ALAS preparation was concentrated, using Centricon-30 concentrators or Amicon ultrafiltration cells with a YM30 or YM10 membrane.

Spectroscopic Methods: UV−Visible and CD Spectra. Absorption spectra were recorded with a 1-cm cell, using a Shimadzu UV 2100U spectrophotometer. ALAS wild-type and mutant samples (10−20 μM) were dialyzed for 6 h against three changes of buffer A containing PLP at a concentration stoichiometric with that of the enzyme plus 10%. The dialyzed samples were centrifuged to remove any denatured protein. The absorption spectra were then recorded on the supernatant solutions, using the dialysis buffer as reference.

CD spectra were obtained using a Jasco J710 spectropolarimeter calibrated for both wavelength maxima and signal intensity using an aqueous solution of *d*-10-camphorsulfonic acid (Chen & Yang, 1977). Visible spectra (20−60 μM enzyme), recorded over the wavelength range of 350−500 nm, were obtained using a sealed microcell of 1 cm path length and a total volume of 90 μL. UV spectra (2−10 μM enzyme) were recorded over the wavelength range of 200−270 nm using a cylindrical cell of 0.1 cm path length and a total volume of 300 μL. Visible CD spectra obtained during apoenzyme titrations (8−15 μM enzyme) with PLP were recorded using a cylindrical cell of 1 cm path length and a total volume of 600 μL. All spectra were obtained at 25 °C using extensively filtered or centrifuged samples and corrected for buffer contributions and are expressed in terms of molar ellipticity.

Determination of K_d: the Equilibrium Constant for Dissociation of PLP from ALAS. The K_d values were determined by CD spectrometric titration of the apo ALAS enzyme with PLP. ALAS wild-type and the mutant forms were in buffer A minus PLP at a concentration range of 8−15 μM. A series of PLP stocks were prepared, and a minimum amount of each was added to the enzyme cuvette to achieve the desired PLP concentration, so the dilution of the protein sample was less than 5% and ignored. CD spectra in 400−500 nm region were recorded after each addition of PLP. The changes in the spectra were used to calculate the K_d values. K_d is defined as

$$K_d = ([\mathrm{ALAS}]_{apo}[\mathrm{PLP}]_{ub})/[\mathrm{ALAS}]_{holo} \quad (1)$$

where $[\mathrm{ALAS}]_{apo}$ and $[\mathrm{PLP}]_{ub}$ are concentrations of the apo ALAS and unbound PLP cofactor, respectively, and $[\mathrm{ALAS}]_{holo}$ represents the concentration of the holo ALAS. The ratio R of bound PLP to total PLP was derived as

$$R = (1/2)\{1 + K_d/[\mathrm{PLP}]_t + [\mathrm{ALAS}]_t/[\mathrm{PLP}]_t - \sqrt{(1 + K_d/[\mathrm{PLP}]_t + [\mathrm{ALAS}]_t/[\mathrm{PLP}]_t)^2 - 4[\mathrm{ALAS}]_t/[\mathrm{PLP}]_t}\} \quad (2)$$

where $[\mathrm{PLP}]_t$ is the total PLP concentration and $[\mathrm{ALAS}]_t$ is the total ALAS concentration.

Changes in the apparent ellipticities at 420 nm (or 400 nm for G142C) were plotted against $[\mathrm{PLP}]_t$, and the theoretical curve was generated to fit the experimental data points. Equation 2 was used to construct the theoretical curve, with K_d in the equation as the variant. The value that represented the best fit of the curve to the data points was chosen as the determined K_d.

Determination of the Thermostability of ALAS. The thermostability of the enzyme was assessed at a protein concentration of 7 μM for the wild-type ALAS and the Gly-144 mutants and 16 μM for the G142C mutant ALAS. The enzyme was heated at a given temperature for 3 min and then rapidly cooled to 0 °C, using a MJ Research MiniCycler. The treated sample was assayed for ALAS activity, which was conducted at 30 °C with the substrate concentrations of 10 μM for succinyl CoA and 100 mM for glycine. The activity obtained from the enzyme treated at 0 °C was assigned as 100%. The temperature needed to achieve 50% activity was defined as $T_{1/2}$ and was used to compare the thermostability of the wild-type ALAS with those of the glycine mutants.

Computer Modeling of the ALAS Glycine Loop. The X-ray structure coordinates of rabbit muscle glycogen phosphorylase *b* (Protein Databank file 9GPB; Barford & Johnson, 1989) were used to model the possible effects of mutations within the homologous glycine loop of ALAS. Molecular modeling was performed using a Silicon Graphics 4D-210GTX computer and the InsightII software package, including Discover (Biosym Inc., San Diego). Amino acid substitutions were made to replace the glycine loop of 9GPB with the corresponding murine ALAS2 sequence: HGAGAG-GTRNI (murine ALAS2, residues 141−151); AGLGNG-GLGRL (rabbit muscle glycogen phosphorylase, 9GPB, residues 129−139).

The glycine loop of the resulting structure was energy minimized, and a dynamics trajectory was computed for the loop region (with the remainder of the molecule fixed) for 120 ps at 300 K. The lowest energy conformational cluster was identified, averaged, and energy minimized using the consistent valence force field to produce the wild-type glycine-loop model. Mutations were introduced and further energy minimization was performed. Within the context of the wild-type model, it was found that for each mutant the conformation of the mutated side chain was constrained to only one feasible set of χ values.

RESULTS

Kinetic Characterization of ALAS Gly-Loop Mutants. Purified glycine-loop mutants were first characterized for kinetic parameters (Table 1). All of the mutants retained activity, although the specific activities were lower than that of the wild-type ALAS. The determined turnover numbers were 43%, 39%, 21%, and 6% of the wild-type value for

Table 1: Kinetic Parameters for Glycine-Loop Mutants of ALAS[a]

enzyme	K_mGly (mM)	K_mSuc (μM)	k_{cat} (h^{-1})	k_{cat}/K_m^{Gly} ($mM \cdot h^{-1}$)	k_{cat}/K_m^{Suc} ($\mu M \cdot h^{-1}$)
WT ALAS	12.5	1.2	1112	89	927
G144A	9.3	0.64	479	52	748
G144S	11.9	1.2	431	36	359
G144T	6.2	1.9	230	37	121
G142C	52.2	2.0	67	1.3	33

[a] Assays were performed at 30 °C in a 1 mL reaction mixture containing 20 mM Hepes, pH 7.2, 1 mM α-ketoglutarate, 1 mM NAD^+, 3 mM $MgCl_2$, 0.25 mM thiamin pyrophosphate, 0.25 unit of α-ketoglutarate dehydrogenase, 5−200 mM glycine, and 0.5−30 μM succinyl-CoA. The enzyme concentration was 0.5−0.9 μM for the ALAS wild-type and Gly-144 mutant forms and 12.7 μM for G142C. ALAS activity was determined by recording the time−course absorbance increase at 340 nm, which reflects the enzymatic production of CoASH. The experimental data were analyzed using the Shimadzu kinetics software program. Abbreviations: K_m^{Gly}, K_m for glycine; K_m^{Suc}, K_m for succinyl-CoA; WT, wild type.

the G144A, G144S, G144T, and G142C mutants, respectively. However, the K_m values of the mutants for both substrates were within a magnitude of the wild-type value in all but one case. The exception was K_m^{Gly} for G142C, which exhibited a 4-fold increase, as compared with that of the wild-type enzyme. The overall catalytic efficiency of G142C with respect to glycine and succinyl-CoA was only 1.5% and 3.6%, respectively, of that of the wild-type enzyme. The Gly-144 mutants also showed lower k_{cat}/K_m for both substrates, ranging from a 42−60% decrease for glycine and a 20−87% decrease for succinyl-CoA, when compared to the wild-type enzyme.

UV-Visible and CD Spectral Properties. The absorption spectra of the wild-type ALAS and the G144A, G144S, G144T, and G142C mutants exhibited absorbance maxima at 278 and 420 nm (Figure 1, panels A and B). The wild-type and Gly-144 mutant enzymes also presented a third absorbance maximum at 330 nm, which was not present in G142C. Instead, G142C showed a shoulder around 340 nm. When PLP was removed from ALAS, the apoenzymes only displayed absorbance maxima at 278 nm (Figure 1, panel C). The 278 nm absorbance maximum corresponds to the protein absorbance maximum (Ferreira & Dailey, 1993), while the 420 nm band represents the internal aldimine formed between K313 in ALAS and the PLP cofactor (Ferreira et al., 1993). Further, the absorbance maxima at 330 and 420 nm, as have been well established in other PLP-dependent enzymes (Yano et al., 1992), are likely to reflect different ionization states of the imine nitrogen of the active site internal aldimine bond: the 420 nm absorbance maximum represents the protonated form of the internal aldimine, while the 330 nm absorbance maximum corresponds to the unprotonated form. Interestingly, the relative intensity of these two absorbance maxima was different among the mutants and the wild-type ALAS: G144S showed a pattern similar to that of the wild-type enzyme, while in G144A and G144T, the 420 nm absorbance maximum was relatively increased (Figure 1, panel B).

The CD spectra of the wild-type and mutant enzymes in the visible region are shown in Figure 2. The Gly-144 mutants displayed spectra very similar to that of the wild-type, with a strong positive CD maximum around 420−430 nm, which reflects the asymmetric orientation of the bound PLP at the active site. In contrast, the G142C mutant showed a spectrum significantly different from that of the wild-type enzyme. The 420 nm band was shifted to 380 nm with a diminished maximum compared with the wild type, and a negative CD maximum was observed at 420 nm (Figure 2, panel A). This result suggests that the PLP binding mode in the active site of G142C was different from that of the wild-type ALAS. For the apoenzymes of the wild-type and mutants, no CD maxima were detected in the visible region (Figure 2, panel B).

To verify whether mutations at Gly-142 or Gly-144 introduced substantial changes in secondary structure, CD spectra in the far-UV region (200−270 nm) were recorded for the wild-type and mutant enzymes. As shown in Figure 3, both holoenzymes and apoenzymes of all forms of ALAS displayed very similar CD spectra. These data suggest that neither the mutations nor the removal of the cofactor resulted in gross changes in the overall conformation of the ALAS protein.

Binding Affinity of Gly-Loop Mutants for PLP Cofactor. Titration of ALAS apoenzymes with PLP resulted in a series of visible CD spectra with progressive intensity increase in the visible region (Figure 4, inset), which represents the process of reconstitution of ALAS with PLP. This reconstitution process correlated well with the gain of enzymatic activity (data not shown). Changes of the CD intensity at 420 nm (or 400 nm for G142C) were plotted against PLP concentrations for each enzyme sample. Theoretical saturation curves were then generated, from which the equilibrium constant for dissociation of PLP from ALAS, K_d, was determined for the wild-type and mutant ALAS enzymes (Figure 4). Table 2 summarizes the obtained K_d values. Wild-type ALAS exhibited the highest affinity for PLP, while lower affinity was observed in all of the four glycine mutants, with the K_d determined to be 8-, 8.5-, 24.5-, and 15-fold higher than the wild-type values for G144S, G144A, G144T, and G142C, respectively.

Thermostability of ALAS Variants. Thermostability experiments were performed to determine the relative stability of ALAS wild-type and mutant enzymes. The enzymatic activity as a function of heat treatment is illustrated in Figure 5. All of the mutants were less stable than the wild-type enzyme. The thermotransition temperature $T_{1/2}$, which is defined as the temperature that results in 50% loss of activity, was determined to be 57, 53.5, 54, 53.5, and 52 °C for the wild type, G144A, G144S, G144T, and G142C, respectively.

Computer Modeling of the ALAS Gly-Loop. No three-dimensional ALAS structure has yet been determined. Consequently, we used glycogen phosphorylase *b* as the basis for molecular modeling in the present study because of the sequence similarity between corresponding glycine loops in the two proteins. In GPB the 10-residue glycine loop is adjacent to PLP, and significant interactions have been noted by McLaughlin et al. (1984). GPB and ALAS both contain PLP as the cofactor which participates in catalysis at the active site, although the catalytic mechanisms differ. However, this does not rule out the possibility that the two enzymes share a common structure in the particular glycine-loop region, as the primary sequences of both enzymes in this region are very similar and the proposed function of the motif is the same.

Interactions in the Wild-Type Model. In the model (Figure 6, panel A), PLP interacts with two residues at the C-terminus of the glycine loop. The side chain of Arg-149 is positioned

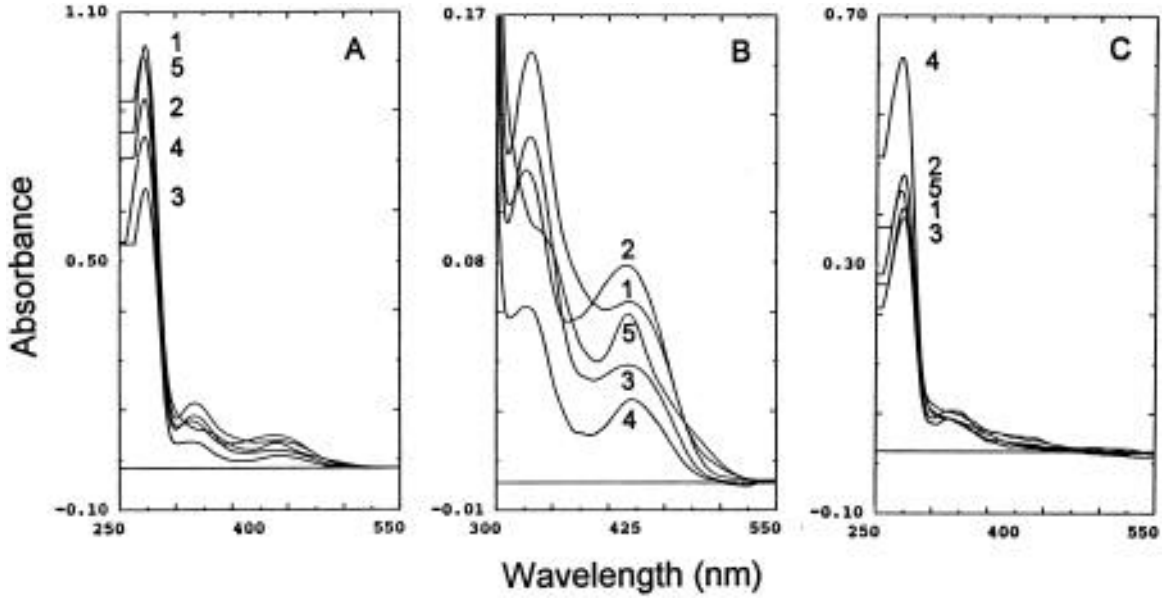

FIGURE 1: Absorption spectra of ALAS G142- and G144-directed mutants. Spectra were recorded in 20 mM potassium phosphate buffer, pH 7.2, as described under Methods. Panel A: ALAS holoenzyme of the wild-type and mutant forms. Curves: 1, wild type (18.2 μM); 2, G144A (15.9 μM); 3, G144S (12.0 μM); 4, G144T (14.3 μM); 5, G142C (17.7 μM). Panel B: absorption spectra of PLP bound to ALAS (enlargement of the visible region in panel A). Panel C: absorption spectra of ALAS apoenzymes. Concentrations: wild type (7.0 μM); G144A (7.9 μM); G144S (6.7 μM); G144T (11.3 μM); G142C (7.5 μM). Number labels in panels B and C are as in panel A.

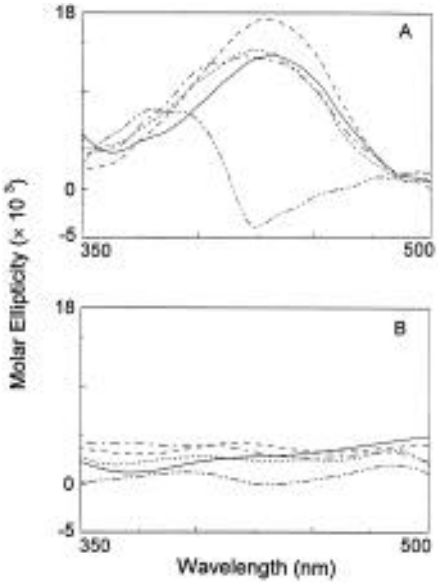

FIGURE 2: CD spectra of PLP bound to the active site of ALAS enzymes. Spectra were recorded in 20 mM potassium phosphate buffer, pH 7.2. Panel A: holoenzymes. Curves: —, wild type (62 μM); ---, G144A (44 μM); — —, G144S (51 μM); — - —, G144T (21 μM); — -- —, G142C (24 μM). Panel B: apoenzymes at the following protein concentrations: wild type, 7.1 μM; G144A, 8 μM; G144S, 8 μM; G144T, 11.3 μM; G142C, 15 μM. Symbols are as in panel A.

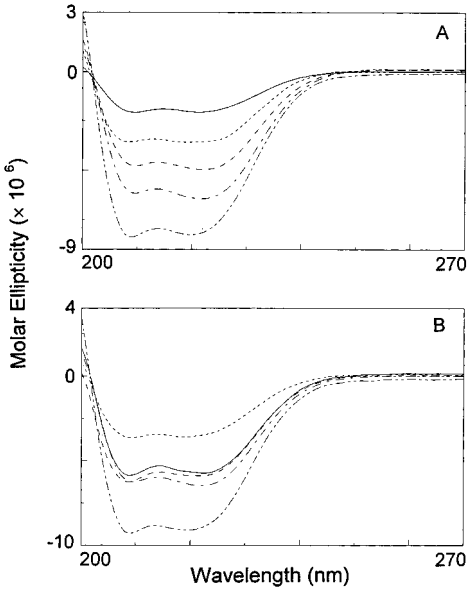

FIGURE 3: CD spectra of ALAS wild-type and mutant enzymes in the far-UV region. Spectra were recorded in 20 mM potassium phosphate buffer, pH 7.2. Panel A: holoenzymes. Curves: —, wild type (10 μM); ---, G144A (1.8 μM); — —, G144S (10.9 μM); — - — , G144T (8.6 μM); — -- —, G142C (3.9 μM). Panel B: apoenzymes at the following protein concentrations: wild type, 1.5 μM; G144A, 2.9 μM; G144S, 3.6 μM; G144T, 7.1 μM; G142C, 1.8 μM. Symbols are as in panel A.

close to the phosphate group of PLP (4.6 Å). The side chain of this residue forms hydrogen bonds to the peptide carbonyl groups of Asn-150 and Gly-147, which possibly serve to position the side chain relative to PLP. In ALAS this critical arginine residue (Gong & Ferrreira, 1995) is one residue prior to the corresponding arginine of the glycine loop of GPB, although in GPB the arginine does not interact directly with PLP (McLaughlin et al., 1984). The side chain of Asn-150 forms a hydrogen bond to the hydroxyl group of PLP in the wild-type model. The side chain of Ile-151 is located away from PLP. The remainder of the glycine loop leads away from the PLP, with the closest side chain (Ala-145, see below) 6 Å distant.

Relating Changes in Model Mutant Structures to Changes in Catalytic and Binding Properties. Introduction of the mutations G142C, G144A, G144S, and G144T individually into the wild-type model structure, and subsequent energy minimization, resulted in changes in the conformation of the glycine loop that were examined for possible correlations with observed changes in catalytic and PLP-binding properties compared to the wild-type enzyme. In the models, the extent of structural changes induced by the mutations was

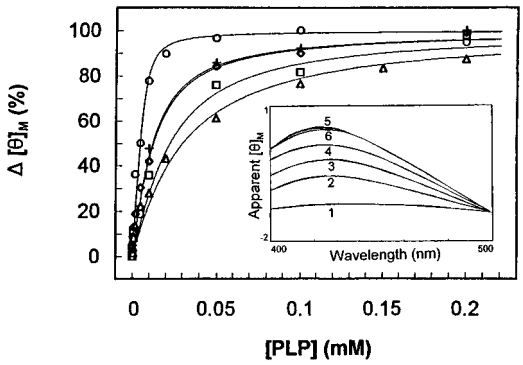

FIGURE 4: CD titration of apo ALAS enzymes with PLP at pH 7.2, 25 °C. The titration was performed by recording CD spectra of ALAS enzymes in the presence of 0−1 mM PLP. Apoenzymes were prepared in 20 mM potassium phosphate buffer, pH 7.2. Changes in the apparent molar ellipticities at 420 nm were plotted as a function of [PLP] in the sample solution for each enzyme. Theoretical curves were generated to fit the data points; K_d values were determined according to the best fitted curves. Symbols: ○, wild type (7.1 μM); ◇, G144A (8.0 μM); +, G144S (8.0 μM); △, G144T (11.3 μM); □, G142C (15.0 μM). Inset: titration data for the wild-type ALAS. The spectra were recorded in the presence of 0 (curve 1), 2 (curve 2), 5 (curve 3), 20 (curve 4), 50 (curve 5), and 200 (curve 6) μM PLP. Some data points were omitted for clarity.

Table 2: PLP Dissociation Constants for ALAS Wild-Type and Gly-Loop Mutants[a]

enzyme	K_d (μM)	enzyme	K_d (μM)
WT ALAS	1	G144T	24.5
G144A	8.5	G142C	15
G144S	8		

[a] K_d, the equilibrium constant for dissociation of PLP from ALAS, was determined by CD titration of the apo ALAS enzymes with PLP in 20 mM potassium phosphate buffer at 25 °C, pH 7.2. The K_d values were calculated from the data reported in Figure 4. Abbreviation: WT, wild type.

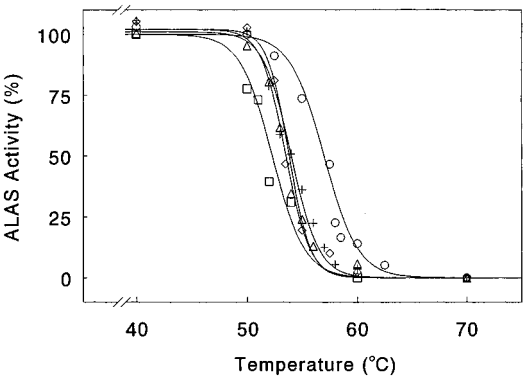

FIGURE 5: Thermostability of ALAS wild-type and glycine mutant enzymes. ALAS activities were determined after preincubating the enzyme samples at given temperatures for 3 min. The activity obtained with the sample treated at 0 °C was defined as 100%. Changes in the activity were plotted against temperatures at which the samples were treated. Symbols: ○, wild type; ◇, G144A; +, G144S; △, G144T; □, G142C. Thermotransition temperature $T_{1/2}$, the temperature of which there is a 50% decrease in enzymatic activity, was determined to be 57, 53.5, 54, 53.5, and 52 °C for the wild-type ALAS, G144A, G144S, G144T, and G142C, respectively.

restricted to the residues from His-141 to Gly-146. Mutation G142C was the most disruptive of PLP binding and catalysis (see above). This was not due to the perturbation of the remainder of the glycine loop, since the G142C mutant structure was most similar to the wild type in all respects except for the presence of the cysteinyl side chain. In the model the side chain is directed toward the PLP, but too distant for direct interaction. Instead, it protrudes into a space between the wild-type loop and PLP (Figure 6, panel B). We therefore suggest that this space is important for cofactor binding and/or substrate processing. A similar effect was observed with the Gly-144 mutants, in which the methyl group of Ala-145, and to a lesser extent all of Ala-145 to Gly-146, was pushed into a space adjacent to that occupied by the side chain of Cys-142, and also directed toward PLP. The closest approach of the methyl side chain of Ala-145 to PLP for these mutations is listed below and correlates well with the experimentally determined extent of PLP binding and catalytic disruption for these mutations: wild type, 6.05 Å; G144A, 5.97 Å; G144S, 5.64 Å; G144T, 4.96 Å.

DISCUSSION

The work reported here completes a series of studies on the effects of mutations of two glycines in a conserved glycine-rich sequence in ALAS. We have proposed that this glycine-rich sequence forms a loop structure and constitutes part of the cofactor binding pocket in the enzyme active site. The results from this study are discussed below in the light of previous mutagenesis experimental data (Gong & Ferreira, 1995).

We have noticed that a glycine-rich motif (141-HGAGAG-GTRNI in murine ALAS2) is conserved in all ALAS enzymes with available sequences (Gong & Ferreira, 1995). To address the importance of the motif in relation to the function of ALAS, we previously performed the informational content analysis of each residue within the loop region (Gong & Ferreira, 1995). From a 20% random library of the 11-residue motif, most positions were found to be able to accommodate several other amino acids as functional replacements; however, Gly-142 and −144 were found to tolerate Ala substitution only, while Arg-149 was conserved in all of the functional mutants identified. The results suggest that the latter three residues play important role(s) in ALAS function. In an effort to further challenge the stringency of the two glycine positions, we constructed a 100% random library specifically for Gly-142 and −144. As the result, G142C, G144A, G144S, and G144T were identified as the functional replacements (Gong & Ferreira, 1995).

In the current study, we have demonstrated that mutations of Gly-142 with Cys and Gly-144 with Ala, Ser, and Thr disturbed both PLP binding and catalysis. From the absorbance spectra, the presence of an absorbance maximum around 420 nm in all four mutants indicates that they all form the Schiff base linkage between the aldehyde group of PLP and the ϵ-amino group of Lys-313 in the enzyme, as reported for the wild-type ALAS (Figure 1; Ferreira & Dailey, 1993). However, although the Gly-144 mutants largely assume the wild-type cofactor binding mode, the asymmetric orientation of the bound cofactor was altered in G142C, as verified by visible CD spectra (Figure 2). Both positive and negative Cotton effects have been observed in a number of PLP-dependent enzymes (Ferreira et al., 1995; Hayashi et al., 1993; Lu et al., 1993; Yano et al., 1992; Marceau et al., 1990; Iwamoto et al., 1984; Yonaha et al., 1975, 1983; Dunathan, 1971). As PLP is not a chiral molecule, the Cotton effect of bound cofactor in the active

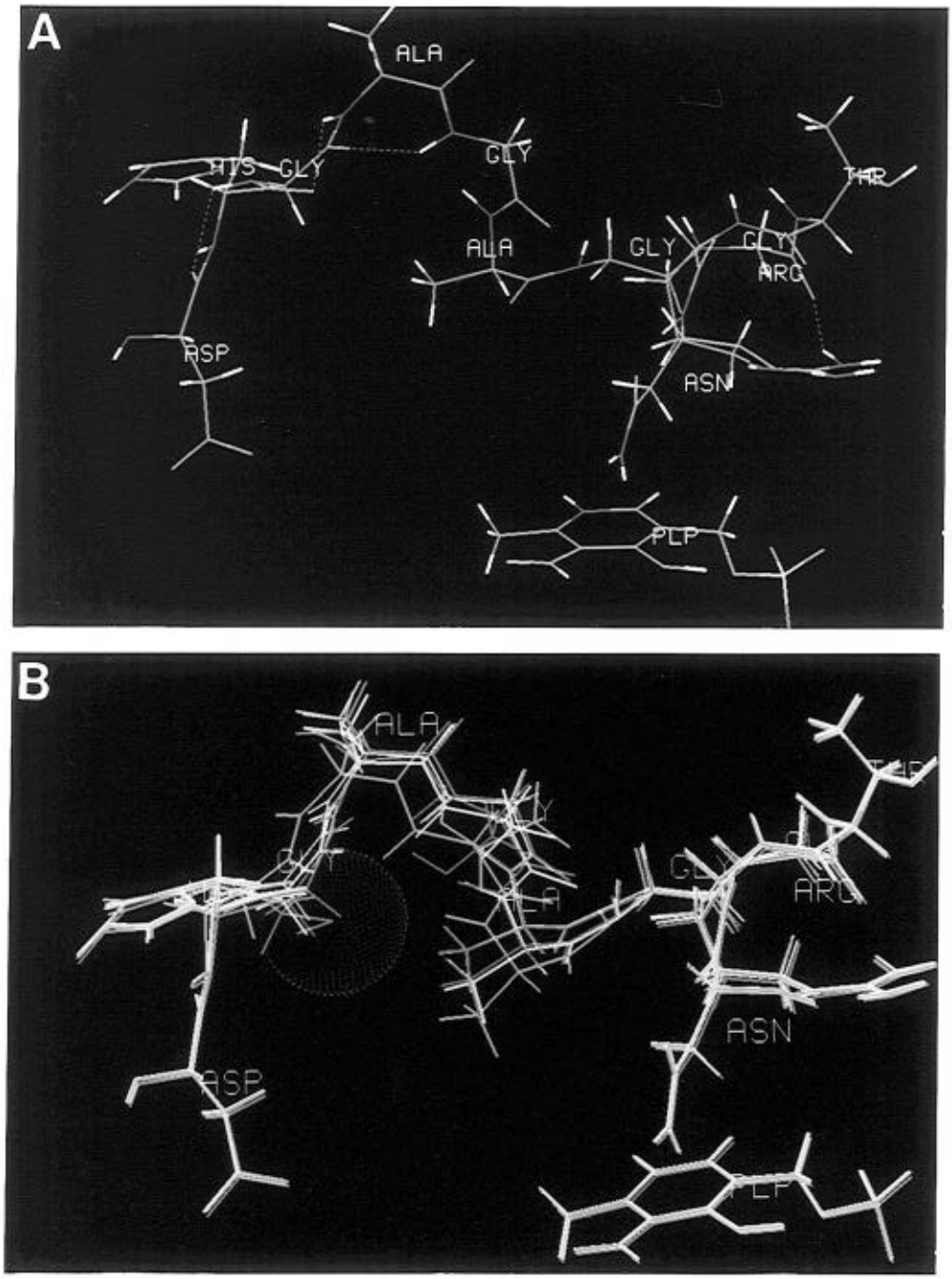

FIGURE 6: Structural models of the ALAS glycine loop. Panel A: Model of the three-dimensional structure of the wild-type ALAS glycine loop based on the crystal structure of glycogen phosphorylase *b*. Carbon atoms are colored green, nitrogen atoms are in blue, hydrogen atoms are in white, oxygen atoms are in orange, and the phosphate atom is in pink. Hydrogen bonds are displayed by dotted lines in green. Panel B: Superposition of the models of ALAS glycine-loop mutants with that of the wild type to illustrate the effects of the mutations. The wild type model is in pink, the G142C mutant model in orange, the G144A mutant model in green, the G144S mutant model in yellow, and the G144T mutant model in blue. Note that the side chain of Ala-145 is pushed toward PLP progressively as Gly-144 is aggressively mutated to Ala, Ser, and Thr. The van der Waals radius of the side chain of the cysteine residue in the G142C mutant is represented as a dotted ball in orange, illustrating the bulkiness of the mutation.

site must result from certain asymmetric distortion of the PLP molecule through interaction with the enzyme. One possible such distortion, as pointed out by Dunathan (1971), might result from the rotation of the $C_4' = N$ group around the C_4-C_4' bond that moves the group out of the plane of the pyridine ring. However, a clear relationship between the mode of the PLP binding and the Cotton effect has not yet been elucidated. Nevertheless, the fact that G142C presents a visible CD spectrum distinct from that of the wild-type pattern provides evidence to suggest that its cofactor binding mode is different from the wild-type arrangement.

Mutations of the glycines also affect enzyme catalysis, as revealed by the kinetic data (Table 1). The selected glycine-loop functional mutants displayed lower k_{cat} values in all cases and a higher K_m^{Gly} value in G142C. This indicates that both the catalysis and the binding of glycine substrate were affected in the mutants, suggesting that perturbations in the glycine loop may induce conformational changes, and/or alterations of cofactor orientation, which affect residues involved in both catalysis and substrate binding.

The characterized mutations of the two glycines caused an 8−24.5-fold decrease in the affinity of PLP for ALAS;

moreover, the increase in K_d value correlates well with the bulkiness of the side chains in mutations at Gly-144 (Table 2). The side chains of the mutations might sterically interfere with the cofactor binding; alternatively, the mutations might induce conformational changes that perturb the PLP-binding residue(s). To investigate the possible structural changes at the glycine loop upon the mutations at the two glycine positions, we performed computer modeling of the ALAS glycine loop, using glycogen phosphorylase *b* as the structural template. In the structural model of the G142C glycine loop, the mutation does not introduce any significant conformational changes to the loop motif; however, the bulky side chain of the Cys is extended into a space forward of the 141−144 turn, slightly pushing toward PLP (Figure 6, panel B). The result suggests that the region forward of the loop might be important for PLP binding and/or substrate binding. The presence of the bulky sulfhydryl group might alter the structure in this region so as to perturb the group(s) that participate(s) in cofactor binding and/or catalysis. However, without a crystal structure of ALAS, it is not clear exactly how the structure is altered upon the G142C mutation and how this has led to the experimentally observed effects, namely, the changes in the asymmetric orientation of the bound PLP, the decrease in the binding affinity, the affected binding of the glycine substrate, and the decrease in the catalytic efficiency (Figures 2 and 4; Tables 1 and 2). As to the Gly-144 mutants, the models reveal that the mutations disturb the loop structure in a manner such that the methyl group of Ala-145 is pushed toward the PLP. A correlation exists between the shortness of the distance of the methyl side chain to PLP and the aggressiveness of the mutations at the Gly-144 position. This, in turn, relates well with the severity of the kinetic and cofactor binding effects (Figures 4 and 6; Tables 1 and 2). Thus this glycine residue seems to be structurally important for the cofactor binding pocket. Replacing with any larger side chains may sterically hinder the motif from assuming the proper conformation and result in the disturbed cofactor binding at the enzyme active site. Once again, a better understanding of the exact contribution(s) of this glycine residue, and the entire glycine loop in general, to the ALAS cofactor binding and catalysis will have to await the availability of the ALAS three-dimensional structure.

Importantly, the glycine loop has been identified in other PLP-dependent enzymes as a cofactor binding motif. In addition, the consensus sequence GXGXXG, where X can be any residue, is well established as a "phosphate gripper" in many nucleotide-binding proteins (Branden & Tooze, 1991; Saraste et al., 1990; Swindells, 1993; Wierenga et al., 1983). Among the PLP−enzymes with available three-dimensional structures, a glycine-rich loop was found at the cofactor-binding site in glycogen phosphorylase *b* (with the sequence 130-GLGN**GG**LG; Oikonomakos et al., 1987; McLaughlin et al., 1984), tryptophan synthase (232−**GGGSNA**IG; Hyde et al., 1988), aspartate aminotransferase (107-G**GT**GAL; Kirsch et al., 1984), tyrosine phenol-lyase (98-Q**GR**GAE; Antson et al., 1993), dialkylglycine decarboxylase (110−**TG**AESN; Toney et al., 1995), and *Lactobacillus* 30a ornithine decarboxylase (195-LG**GSS**N; Momany et al., 1995). The residues in bold in each loop structure interact with the cofactor through hydrogen bonding and/or van der Waals contacts. In addition, similar glycine-loop structures were also identified in several threonine dehydratases (Datta et al., 1987) and the D-serine dehydratase (Marceau et al., 1990). Notably, in the latter case the authors reported that the conserved glycines in the loop were not directly used to bind PLP, although the glycine loop is spatially adjacent to the cofactor. Importantly, Grishin et al. (1995) recently classified PLP-dependent enzymes into 7-fold types, among which the enzymes with known structures cover 3-fold types. The authors pointed out that, throughout these 3-fold types, there are two regions in the PLP-binding sites that are conserved: a lysine residue which forms the Schiff base with the cofactor and a glycine-rich loop which interacts with the PLP phosphate group. In their report, ALAS was categorized in fold type I, together with the following enzymes with known structures: aspartate aminotransferase, dialkylglycine decarboxylase, tyrosine phenol-lyase, and prokaryotic ornithine decarboxylase. Members of fold type I primarily consist of enzymes classified as α-family by other authors (Alexander et al., 1994), the designation derived from the common character that members of this family primarily catalyze the transformations of amino acid substrates in which the covalency changes occur at the same α-carbon that forms the aldimine linkage to the cofactor through its amino group. Interestingly, recent views have suggested that α-family enzymes are likely to adopt an overall similar folding pattern, despite the fact that little homology exists among the primary sequences (John, 1995; Toney et al., 1995).

In summary, mutations of Gly-142 by Cys and Gly-144 by Ala, Ser, and Thr within a conserved glycine-rich sequence in ALAS result in considerable decreases in PLP-binding affinities and catalytic efficiencies of the enzyme. G142C also exhibits an altered PLP-binding mode as revealed by the visible CD spectrum. The experimental evidence, along with the results of computer modeling of the glycine-loop structures, strongly suggests that the glycine loop in ALAS constitutes part of the cofactor-binding pocket in the active site of the enzyme.

ACKNOWLEDGMENT

We thank Mr. D. Tan for providing the pDT6 construct. We are grateful to Dr. Steven G. Lloyd at Emory University for providing the computer program for calculating the K_d values. The suggestion of performing computer modeling on the ALAS glycine loop from Dr. Jack F. Kirsch at University of California at Berkeley is gratefully acknowledged. Finally, we thank Drs. R. Franco, P. Gunaratne, A. Pereira, and P. Tavares, Mr. G. A. Hunter, and Mr. D. Tan for suggestions on this project and for critical reading of the manuscript.

REFERENCES

Alexander, F. W., Sandmeier, E., Mehta, P. K., & Christen, P. (1994) *Eur. J. Biochem. 219*, 953−960.

Antson, A. A., Demidkina, T. V., Gollnick, P., Dauter, Z., Von Tersch, R. L., Long, J., Berezhnoy, S. N., Phillips, R. S., Harutyunyan, E. H., & Wilson, K. S. (1993) *Biochemistry 32*, 4195−4206.

Barford, D., & Johnson, L. N. (1989) *Nature 340*, 609−616.

Bossemeyer, D. (1994) *Trends Biochem. Sci. 19*, 201−205.

Branden, C., & Tooze, J. (1991) in *Introduction to Protein Structure* (Branden, C., & Tooze, J., Eds.) pp 141−159, Garland, New York.

Chen, G. C., & Yang, J. T. (1977) *Anal. Lett. 10*, 1195−1207.

Datta, P., Goss, T. J., Omnaas, J. R., & Patil, R. V. (1987) *Proc. Natl. Acad. Sci. U.S.A. 84*, 393−397.

Dunathan, H. C. (1971) *Adv. Enzymol. 35*, 79−134.
Ferreira, G. C., & Dailey, H. A. (1993) *J. Biol. Chem. 268*, 584−590.
Ferreira, G. C., & Gong, J. (1995) *J. Bioenerg. Biomembr. 27*, 151−159.
Ferreira, G. C., Neame, P. J., & Dailey, H. A. (1993) *Protein Sci. 2*, 1959−1965.
Ferreira, G. C., Vajapey, U., Hafez, O., Hunter, G. A., & Barber, M. J. (1995) *Protein Sci. 4*, 1001−1006.
Gong, J., & Ferreira, G. C. (1995) *Biochemistry 34*, 1678−1685.
Grishin, N. V., Phillips, M. A., & Goldsmith, E. J. (1995) *Protein Sci. 4*, 1291−1304.
Hayashi, H., Mizuguchi, H., & Kagamiyama, H. (1993) *Biochemistry 32*, 812−818.
Hunter, G. A., & Ferreira, G. C. (1995) *Anal. Biochem. 226*, 221−224.
Hyde, C. C., Ahmed, S. A., Padlan, E. A., Miles, E. W., & Davies, D. R. (1988) *J. Biol. Chem. 263*, 17857−17871.
Iwamoto, R., Imanaga, Y., & Soda, K. (1984) *J. Biochem. 95*, 13−18.
John, R. A. (1995) *Biochim. Biophys. Acta 1248*, 81−96.
Jordan, P. M. (1991) in *Biosynthesis of Tetrapyrroles* (Jordan, P. M., Ed.) pp 1−66, Elsevier, Amsterdam.
Kirsch, J. F., Eichele, G., Ford, G. C., Vincent, M. G., & Jansonius, J. N. (1984) *J. Mol. Biol. 174*, 497−525.
Laemmli, U. K. (1970) *Nature 227*, 680−685.
Lu, Z., Nagata, S., McPhie, P., & Miles, E. W. (1993) *J. Biol. Chem. 268*, 8727−8734.
Marceau, M., Lewis, S. D., Kojiro, C. L., Mountjoy, K., & Shafer, J. A. (1990) *J. Biol. Chem. 265*, 20421−20429.
McLaughlin, P. J., Stuart, D. I., Klein, H. W., Oikonomakos, N. G., & Johnson, L. N. (1984) *Biochemistry 23*, 5862−5873.
Momany, C., Ghosh, R., & Hackert, M. L. (1995) *Protein Sci. 4*, 849−854.
Oikonomakos, N. G., Johnson, L. N., Acharya, K. R., Stuart, D. I., Barford, D., Hajdu, J., Varvill, K. M., Melpidou, A. E., Papageorgiou, T., Graves, D. J., & Palm, D. (1987) *Biochemistry 26*, 8381−8389.
Riddle, R. D., Yamamoto, M., & Engel, J. D. (1989) *Proc. Natl. Acad. Sci. U.S.A. 86*, 792−796.
Sanger, F., Nicklen, S., & Coulson, A. R. (1977) *Proc. Natl. Acad. Sci. U.S.A. 74*, 5463−5467.
Saraste, M., Sibbald, P. R., & Wittinghofer, A. (1990) *Trends Biochem. Sci. 15*, 430−434.
Swindells, M. B. (1993) *Protein Sci. 2*, 2146−2153.
Tan, D., & Ferreira, G. C. (1996) *Biochemistry 35*, 8934−8941.
Toney, M. D., Hohenester, E., Keller, J. W., & Jansonius, J. N. (1995) *J. Mol. Biol. 245*, 151−179.
Weber, I. T., Johnson, L. N., Wilson, K. S., Yeates, D. G. R., Wild, D. L., & Jenkins, J. A. (1978) *Nature 274*, 433−437.
Wierenga, R. K., Drenth, J., & Schulz, G. E. (1983) *J. Mol. Biol. 167*, 725−739.
Yano, T., Kuramitsu, S., Tanase, S., Morino, Y., & Kagamiyama, H. (1992) *Biochemistry 31*, 5878−5887.
Yonaha, K., Misono, H., Yamamoto, T., & Soda, K. (1975) *J. Biol. Chem. 250*, 6983−6989.
Yonaha, K., Toyama, S., & Kagamiyama, H. (1983) *J. Biol. Chem. 258*, 2260−2265.

BI961296H